



Technische Universität München
School of Computation, Information and Technology
Bio-Inspired Information Processing

Bachelor's Thesis

Investigation of Cortical Responses to Modulated Noise Stimuli Using fNIRS

Pei-Yi Lin

Date of Submission:
September 17, 2022

Supervisors:
Prof. Dr.-Ing. Werner Hemmert
Dr. Ali Saeedi
M.Sc. Carmen Marie Castañeda González

Abstract

Write your abstract here or use \input{} command.

Acknowledgments

Huge thanks to my friends who volunteered and participated in this study.

Contents

1	Introduction	1
1.1	Motivation	1
1.2	Technical Background	2
1.3	Related Work	4
2	Methods	6
2.1	Study Participants	6
2.2	Probe Design	6
2.3	Acoustic Stimulation during fNIRS Experiment	9
2.4	fNIRS Setup	10
2.5	Data preprocesing	11
3	Results	15
3.1	Participant 3	17
3.2	Participant 5	19
3.3	Participant 6	21
3.4	Participant 7	23
3.5	Participant 4	25
3.6	Participant 8	27
4	Discussion	29
4.1	Waveform Morphology	29
4.2	Regional Analysis	29
4.3	Device Limitation and fNIRS Testing Conditions	30
4.4	Data Processing	31
4.5	Loudness Perception	32
4.6	Audio Stimuli	32
4.7	Language Processing in Human Brains	32
4.8	Laterality of Brain Activation	33
4.9	Depth and Location of Cortical Response	33
4.10	HbR and HbO Data	34

Contents

5 Conclusion and Future Prospectives	35
A Acronym	36
B List of Figures	38
C List of Tables	41
References	45

Chapter 1

Introduction

1.1 Motivation

This research aims to better understand the brain activities of normal-hearing subjects when they are exposed to auditory stimuli of different loudness with the help of functional near-infrared spectroscopy (fNIRS).

In the field of neuro-imaging, although functional magnetic resonance imaging (fMRI) is widely used and provides excellent resolution, it still has many limitations, especially when it comes to hearing research. First of all, that fact that fMRI rooms are noisy makes it difficult to control the auditory stimulation desired due to inevitable environmental noises. In addition, fMRI scans are done in a magnetic field. It has not yet been proved that pregnant women and infants can be safely exposed to an external magnetic field in the fMRI room. For people with hearing disabilities, more specifically cochlear implant patients, going into a fMRI room would not be ideal, either. Although there are already cochlear implants that can be worn to a magnetic field, it is still generally not suggested to wear a piece of metal in a fMRI room.

With fNIRS, we can measure brain activity by using near-infrared light to estimate cortical hemodynamic activities which occur in response to neural activity. It is non-invasive and risk-free. The fNIRS device is portable and works silently. With the cap secured on the head, it is also more resilient to motion artifacts. All these makes it ideal for hearing research. However, it is not yet commonly used in clinical diagnostics due to the lack of understanding of the expected brain activities measured with fNIRS. The spatial resolution is also worse than that of fMRI. Therefore, in this research, we'd like to perform some fNIRS measurement and analyse the fNIRS data under different experiment conditions.

Introduction

If we can utilize fNIRS better so that the technology can be more commonly used in clinical applications, hearing abnormality of patients can be diagnosed earlier. This is especially important for infants or children. There is strong evidence that language development happens in the early stages of one's life Newport [1990], and children may never acquire a language if they have not been exposed to a language before they reach the age of six or seven Clark [2000]. As a result, early identification and intervention of hearing loss can prevent severe linguistic, communicative, psychosocial repercussions Robinshaw [1995] Yoshinaga-Itano et al. [1998]. I find hearing research a meaningful topic. For one, speech is the primary and direct way of human communication. We express ourselves and perceive other people's opinion via speech. For the other, music has always been an important part of my life. Without the ability to hear and listen, neither speech nor music will be possible to be perceived. Therefore, helping other people with hearing disabilities get better diagnosis and treatment is the ultimate goal for this study, and fNIRS is of great potential to help solve the issue.

1.2 Technical Background

The central concept of neuroimaging is dependent on the relationship between oxygen consumption and neuronal activity. Increases in neuronal activity require more glucose and oxygen to be rapidly delivered via the blood stream. Via this hemodynamic response, blood releases glucose and oxygen to active neurons at a faster rate relative to inactive neurons Pelphrey [2013]. By measuring this Blood-oxygen-level-dependent (BOLD) signal, neuroimaging is therefore possible.

Hemoglobin, the protein from inside red blood cells, transports oxygen molecules throughout the body. Higher hemoglobin levels and red blood cell transfusion are associated with higher cerebral oxygen delivery. Different concentration levels of hemoglobin results in a spectral change. The biological tissue has a relatively good transparency for light in the near-infrared region (700-1300nm) Jöbsis [1977]. Therefore, it is possible to transmit sufficient photons *in situ* monitoring.

1.2 Technical Background

The technique of NIRS relies on the Beer-Lambert law Swinehart [1962], which is given by:

$$OD_\lambda = \log\left(\frac{I_0}{I}\right) = \epsilon_\lambda \cdot c \cdot L \quad (1.2.1)$$

OD_λ : a dimensionless factor known as the optical density of the medium.

I_0 : the incident radiation.

I : the transmitted radiation.

ϵ_λ : the molar absorptivity ($mM^{-1} \cdot cm^{-1}$) of the chromophore.

c : the concentration (mM) of the chromophore.

L : length of light path.

The Beer-Lambert law applies for a clear, non-scattering medium. When the law is applied to a scattering medium, e.g. brain tissue, a correction factor should be applied. The factor, called "differential path length factor (DPF)" accounts for the increase in optical path length due to scattering in the tissue. The modified Beer-Lambert law Delpy et al. [1988] is given by:

$$OD_\lambda = \epsilon_\lambda \cdot c \cdot L \cdot B + OD_{R,L} \quad (1.2.2)$$

where $OD_{R,L}$ represents the oxygen-independent light absorption due to scattering in the tissue, and $(L \cdot B)$ is the true mean pathlength traveled by the detected photons. In our case, i.e. CW-NIRS ¹, this mean path length is not known. In a highly scattering medium, the path length of trajectories is longer than the source-detector separation. Nevertheless, one may still estimate the path length within the whole sampling region by multiplying the source-detector distance with a DPF. Assuming $OD_{R,L}$ is constant during a measurement, we may rewrite the previous equation in terms of changes in optical density and changes in concentration as follows:

$$\Delta c = \frac{\Delta OD_\lambda}{\epsilon_\lambda \cdot L \cdot B} \quad (1.2.3)$$

The validity of the above equation depends on how much the DPF, or in this equation "B" varies. Delpy et al. [1988] investigated this question and gave a relation between the DPF and the head diameter. Nonetheless, newer research also provides different ways to estimate the DPF. In the scope of this project, the DPF was calculated from a function of wavelengths and age of the participant Duncan et al. [1996].

¹The Continuous Wave (CW) method relies on the steady illumination of tissue and the detection of the transmitted light intensity. This conceptually and technically simplest form of tissue spectroscopy assesses the overall light attenuation inside the tissue and cannot differentiate effects of scattering and absorption. Source : <https://nirx.net/cwfnirs>

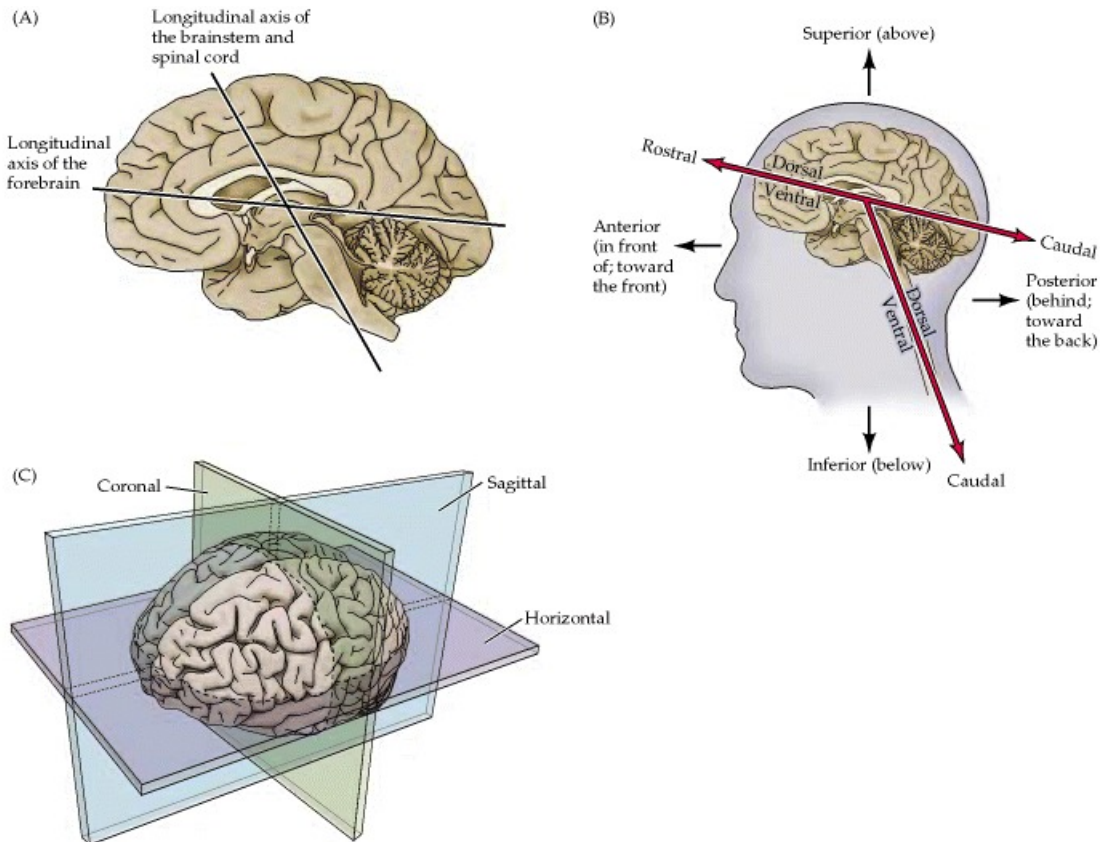
1.3 Related Work

Despite the fact that fNIRS has become a popular neuroimaging method for hearing research, spatial resolution is reduced compared to fMRI and often the exact locations of fNIRS optodes and detailed anatomical information is not known. On top of the limited spatial resolution of fNIRS, the relationship between cortical activation and speech processing is not yet clearly investigated, either. Up till now, there are no standard fNIRS source-detector locations that are generally accepted as being ideal for capturing the cortical activation in response to speech signals. As a result, many research was done to overcome the issues and hopefully enable fNIRS in more clinical applications.

Frost et al. 1999 conducted a fMRI study and found evidence to prove that language processing is strongly left lateralized in both sexes. Belin et al. 2000 also used fMRI in their study and found out that the superior temporal sulcus (STS) showed greater neuronal activity when subjects listened passively to vocal sounds, whether speech or non-speech, than to non-vocal environmental sounds. Shader et al. 2021 conducted a study with fNIRS. They explored broad and restricted regions of interest that are sensitive to detecting cortical activation using fNIRS in response to auditory- and visual-only speech. Their results suggested that temporal regions near Heschl's gyrus may be the most advantageous location in adults for identifying hemodynamic responses to complex auditory speech signals using fNIRS. Pollonini et al. 2013 studied the cortical activation level in response to the speech signals with different levels of intelligibility. fNIRS evidence proved that normal speech evoked the stronger responses within the auditory cortex than distorted speech, and environmental sounds produced the least cortical activation.

This project is based on a previous study Weder et al. [2018]. The authors measured their human subjects with fNIRS when the subjects were given different sound stimuli with different sound pressure levels. In their research, the results showed that fNIRS responses originating from auditory processing areas are highly dependent on sound intensity level. More specifically, higher stimulation levels led to higher concentration changes. Caudal and rostral channels showed different waveform morphologies, reflecting specific cortical signal processing of the stimulus.

1.3 Related Work



Source: <https://www.ncbi.nlm.nih.gov/books/NBK10971/>

Figure 1.1: Some Anatomical Terminology. The terms anterior, posterior, superior, and inferior refer to the long axis of the body, which is straight. Therefore, these terms indicate the same direction for both the forebrain and the brainstem. In contrast, the terms dorsal, ventral, rostral, and caudal refer to the long axis of the central nervous system.

Chapter 2

Methods

2.1 Study Participants

We measured 8 normal hearing people. Participant 8 was given silent stimuli as a comparison. The detailed information about the subjects are listed in the table.

Participant	Gender	Handedness	Race	Hair color	Age (year)
1	F	right-handed	east asian	dark	22
2	M	right-handed	caucasian	blond	18
3	M	left-handed	caucasian	brunet	21
4	F	right-handed	east asian	dark	21
5	M	right-handed	caucasian	blond	26
6	F	right-handed	southeast asian	dark	22
7	M	left-handed	east asian	dark	23
8	M	right-handed	caucasian	blond	22

Table 2.1: Demographic information of the study participants.

2.2 Probe Design

The probes were first designed in AtlasViewer 2.2 Aasted et al. [2015] and the SD GUI interface 2.3. I tried to replicate the probe design as close as possible to the research from Weder et al 2018. However, several modifications need to be made due to device limitations.

First of all, the paper only provided a rough 2D-sketch of their probe design 2.1. The channels were not described in detail. Though there are

2.2 Probe Design

different ways to define the channels, we believe it shouldn't matter as long as the mid-points of the channel correspond to that of the previous research Weder et al. [2018].

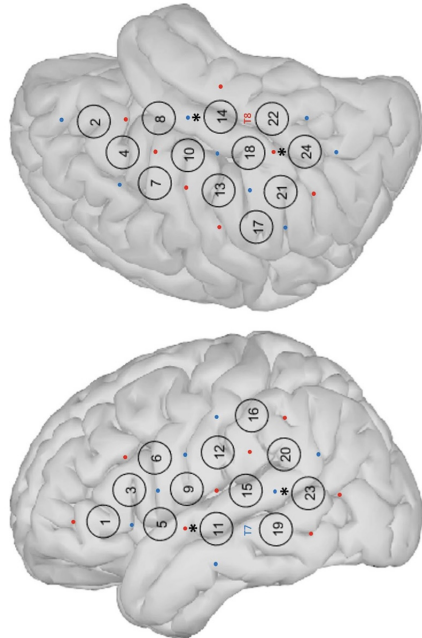


Figure 2.1: Probe design from Weder et al. 2018

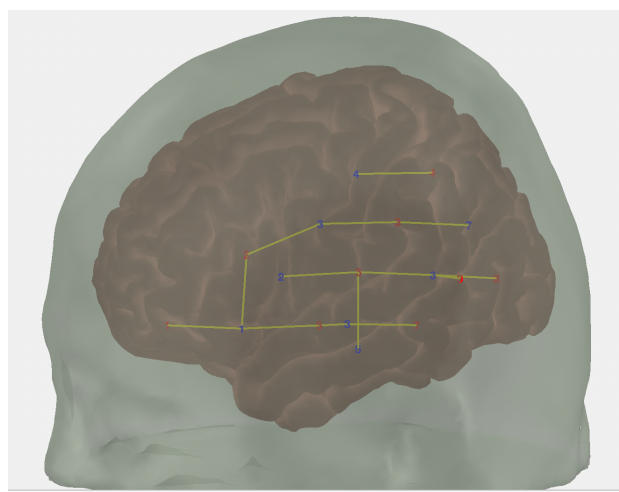


Figure 2.2: Probe design in this research. Shown in AtlasViewer 2015 . The red numbers represent the light sources and the blue numbers represent the detector. Channels are shown in yellow lines.

Methods

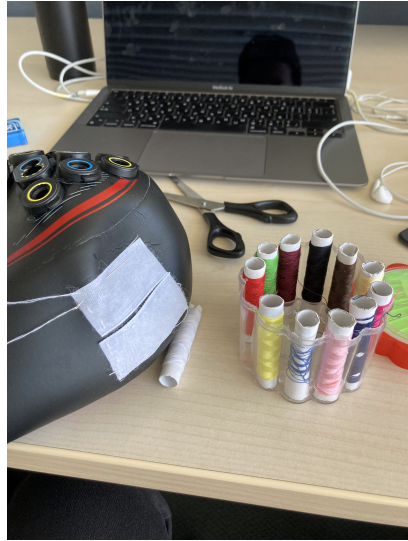


Figure 2.4: Manufacturing process of the cap



Figure 2.5: Finished cap on dummy

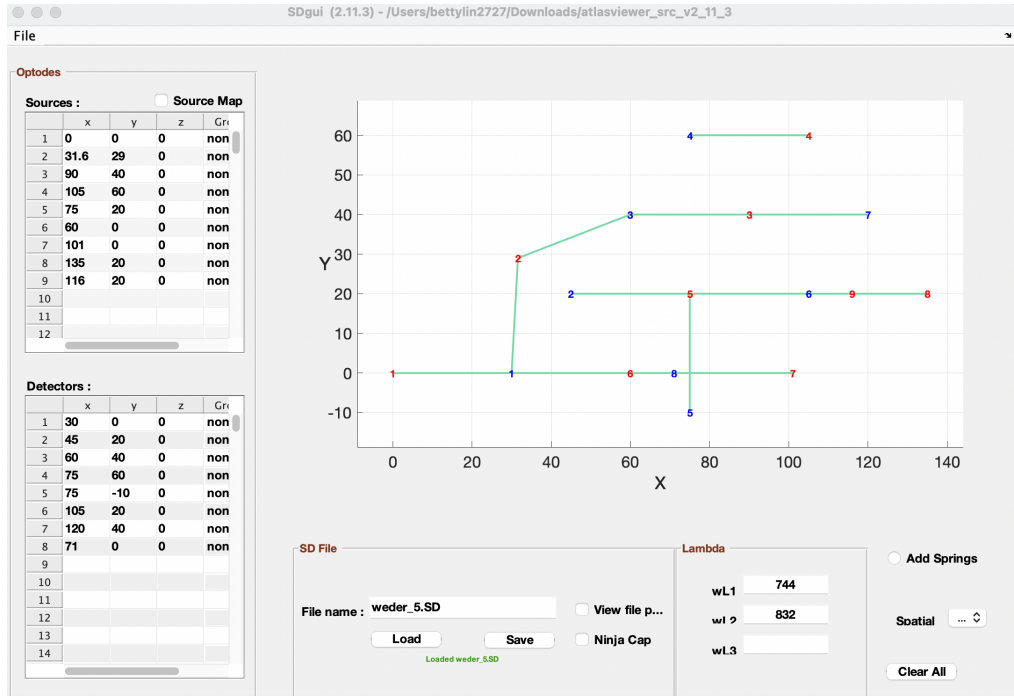


Figure 2.3: SDgui interface and optode coordinates.

Due to device limitations, we only measured one side of the brain. According to previous research Frost et al. [1999] , language processing has

2.3 Acoustic Stimulation during fNIRS Experiment

been predominantly associated to cortical activity in the left hemisphere. As a result, we've decided to focus on the left hemisphere.

The fNIRS device we use also has limited number of sources and detectors. If we'd like to keep the original design, we'd need 9 sources and 9 detectors. However, the device we are using has only 10 sources and 8 detectors. Hence, we shifted one channel around T7 a little bit to the left, so that one less detector is needed. At the end, there were 12 long channels and 2 short channels in our setup.

For the software usage, an .xml file is required. In the .xml file, the sources, detectors, and channels are defined. Different optode templates for different probe design can be stored in one single .xml file. The physical cap was self-made from a swimming cap. With the help of a dummy head model, correct positions of the optodes were marked and holes were drilled accordingly. The mounts were put on the cap on the holes. In order to ensure the correct channels length to be fixed exactly at 30 mm, plastic holders were also placed on the long channels. As for the short channels, the package comes with mounts for short channels. Thus, no plastic holders were needed in the case. The short channels were 11 mm long. The self-made cap turned out to work out well. The contacts between the scalp and the optodes were good thanks to the elastic characteristic of the material.

2.3 Acoustic Stimulation during fNIRS Experiment

Auditory stimuli were delivered binaurally via an audio metric headphone (Sennheiser HD 650). Stimuli consisted of 20-s chunks of the ICRA noise Dreschler et al. [2001].

To begin with, ICRA noise was developed to be used as background noise in clinical tests of hearing aids and possibly for measuring characteristics of non-linear instruments. The signals are based on live English speech from the EUROM database Chan et al. [1995] in which a female speaker is explaining about the system of arithmetical notation. The speech signals were sampled with a sampling rate of 44.1 kHz. By composing the speech signals with well defined spectral and temporal characteristics, the modified signals have long-term spectrums but are completely unintelligible.

We chose to use ICRA noise as stimuli based on several reasons. For one, ICRA noise is broadband amplitude-modulated signal. By selecting a broadband stimulus, broad cortical auditory areas are activated more strongly compared with simple static stimulus. The bandwidth of auditory stimuli is

Methods

positively correlated with the mean percentage signal change and spread of cortical activation Hall et al. [2001]. Previous fMRI study also manifested that more complex auditory stimuli elicit greater response in most parts of the auditory cortes Belin et al. [2002]. For the other, ICRA noise is a well-known and accessible stimulus. It is also considered as an international de facto standard for hearing research. In this way, our results can be comparable with other researches.

As for choosing different sound level pressure, we picked 40 dB, 65 dB, 90 dB, and silent stimulus, i.e. 0 dB. Calibrations were performed using an oscilloscope, a G.R.A.S. Power Module Type 12AK, and an artificial ear (G.R.A.S. 43AA). The artificial ear transform the SPLs (sound pressure levels) into electrical signals, i.e. voltages that can be measured by the oscilloscope. According to the instruction manual of the G.R.A.S. artificial ear, the measured level is $11.19 \left[\frac{mV}{Pa} \right]$ and we know the SPL in dB is defined as

$$SPL[dB] = 20 \cdot \log \frac{P}{P_0}, \text{ where } P_0 \text{ is } 20\mu\text{Pa} \quad (2.3.1)$$

Hence, the relation between SPL and measured voltage should be.

$$V = 20\mu\text{Pa} \cdot 10^{\frac{SPL}{20}} \cdot 10^{\frac{Gain}{20}} \cdot 11.19 \frac{mV}{Pa} \quad (2.3.2)$$

The headphone with the artificial ear were setup together in the sound booth to ensure minimal environmental noise. The output voltages were measured with the oscilloscope. This way, the corresponding amplitude inputs for later MATLAB scripts for the desire SPLs can be determined.

MATLAB and Oxysoft were used during the measurement. In MATLAB, a chunk in the ICRA audio files was selected. It was multiplied with different amplitude levels for 4 SPLs and ramped by a 10-ms Hanning window. In each epoch, all four stimuli (0dB, 40 dB, 65 dB, and 90 dB) were played randomly once. After each stimulus, there was a 25-sec silence rest to wait for the hemodynamic response. For each participant, 8 epochs were conducted. The stimuli were marked with Labstreaminglayer to note which SPL it was. This Labstreaminglayer also acted as an interface between MATLAB and Oxysoft, so that Oxysoft could mark the time for each stimulus in the measurement data correctly in real time.

2.4 fNIRS Setup

The Brite23 was used in this research. It is light weight, has 10 sources and 8 detectors and can support up to 23 channels. The Brite23 fNIRS

2.5 Data preprocesing

device was connected via bluetooth to the PC and the Oxysoft software. For each measurement, the DPF is calculated depends on the age of the participant. The sampling rate was fixed at 50 Hz, for enough resolution but not unnecessary too large in terms of data size.

After the setting in the Oxysoft software was done, the participant would be asked to put on the self-made cap. On each optode position, the hair would be put aside gently with a Q-tip to ensure better contact between the optodes and the scalp. Then, the participants would be asked to put on the headphone and go into the sound booth. The participants were also asked to keep the eyes closed and keep the head still to ensure minimum interference from visual stimulation and motion artifact.

2.5 Data preprocesing

Data preprocessing and analysis was executed in MATLAB (Mathworks, USA) and the Homer3 toolbox. The following steps were executed.

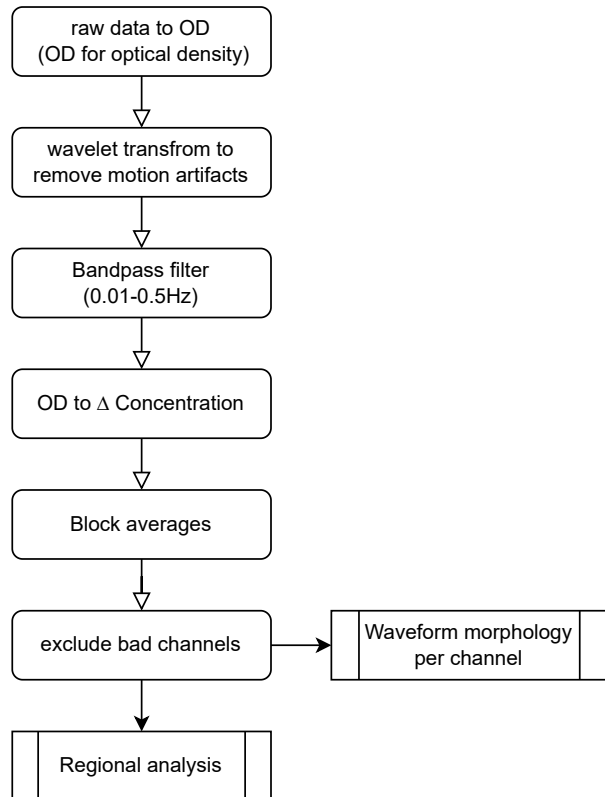


Figure 2.6: Flow Chart of Data Processing

Methods

First, the hemodynamic response was extracted with the Homer3 toolbox. Raw data were converted into optical densities. Motion artifacts were removed by using wavelet transformation of the data. Molavi and Dumont [2012]. We also tried to use principle component analysis (PCA) to remove motion artifact, since PCA has the advantage of faster computation. However, it is also known for tending to remove too much of the activation signal in adults. Wavelet transform on the other hand, takes longer to compute, but it is better at maintaining frequency content. And then, the Homer3 toolbox bandpass filter [0.01 - 0.5 Hz] was used to reduced drift, broadband noise, heartbeat, and respiration artifacts. Changes of concentration of oxygenated and deoxygenated hemoglobin were estimated by applying the modified Beer-Lambert Law Delpy et al. [1988]. In this step, a correction factor, DPF, is used. Although strictly speaking, the DPF should be experimentally obtained with FD-NIRS or TD-NIRS, due to device limitation, it is not possible in this project. Hence, in our research, the DPF was determined by wavelengths of the fNIRS device and age of the participant. Duncan et al. [1996]. With the given literature, the DPF for two wavelength is calculated with the formulas:

$$DPF_{744} = 5.11 + 0.106 \cdot Age[yr]^{0.723} \quad (2.5.1)$$

$$DPF_{852} = 4.67 + 0.062 \cdot Age[yr]^{0.819} \quad (2.5.2)$$

Duncan et al. 1996 developed a broadband radiofrequency-modulated PRS instrument using four wavelengths(690, 744, 807, and 832 nm) which can measure phase shifts through more than 4 cm of brain tissue in less than 1 s. In the study, the modulation frequency was set at 200 MHz, which has been shown theoretically to be a frequency at which phase shift and true mean optical path length are equal Arridge et al. [1992]. By dividing the true mean optical path length with source detector separation, the DPF can be obtained.

The authors also provided mathematical models based on the measurements. The estimated DPF is in a sequential order as the used wavelengths. The shorter the wavelength, the larger the mean DPF they measured. Even though only 4 equations were provided with the above-mentioned 4 wavelengths, and our wavelengths are different then that of the authors used, we are convinced that with the above two equations, we may still get fair estimate of the true DPF in our case.

2.5 Data preprocesing

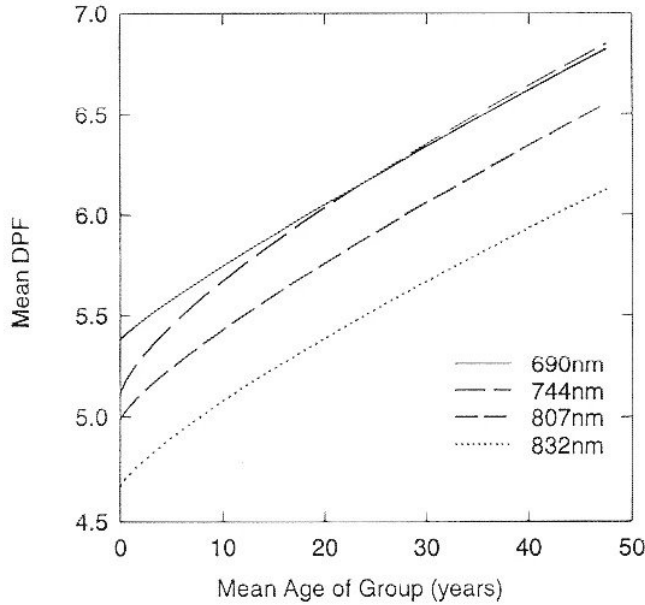


Figure 2.7: Age dependence of DPF. From Duncan et al.

It is important to note that the noise due to motion artifacts, drift, broadband noise, heartbeat, and respiration artifacts need to be processed before the concentration was estimated, according to the previous research Huppert et al. [2009].

Later on, the extracerebral component in long channels should be reduced by using measurements from the short channels as follows: the first principal components from the two short channels were estimated and then multiplied by its coefficient from the GLM (general linear model). However, this is not done in the scope of this research. The coefficient from the GLM were very small. They were of the magnitudes 10^{-16} , whereas the hemodynamic response in the long channels were of the magnitudes 10^{-5} . Hence, we concluded the extracerebral components in our case can be negligible.

Channels with unusable data were excluded here for further analysis. The scalp coupling index (SCI) is a common measure in this case. It is originally described in Pollonini et al. [2013]. In short, the SCI estimates the correlation between the two wavelength channels in the cardiac band as the following:

First, the signal is bandpass-filtered to keep only the cardiac band. In our case, a wide band of [0.5 - 2.5] Hz was chosen. Then, amplitude normalization is performed, and the SCI computation is defined as the absolute cross-correlation value at 0-time lag.

Methods

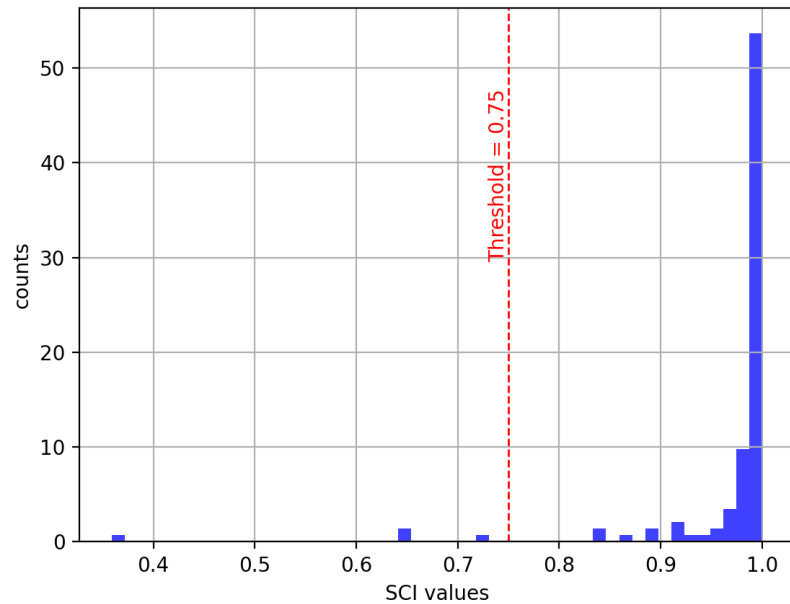


Figure 2.8: Distribution of SCI values.

In this project, only 4 channels failed to reach the threshold = 0.75. In other words, of all the measurements (14 channels per participant, 8 participants in total.) That means over 96% of the measurements passed the SCI threshold.

Chapter 3

Results

From our measurements, the results varied a lot individually. Hence, grand average and further statistical analysis would not be well-applicable. In this section, some of the individual results will be presented, including waveform morphology of the 14-channel measurements for both the HbO and HbR data. In addition, the regional analysis for the HbO data are also included in this section.

First of all, our channels with the optode template are defined as this figure.

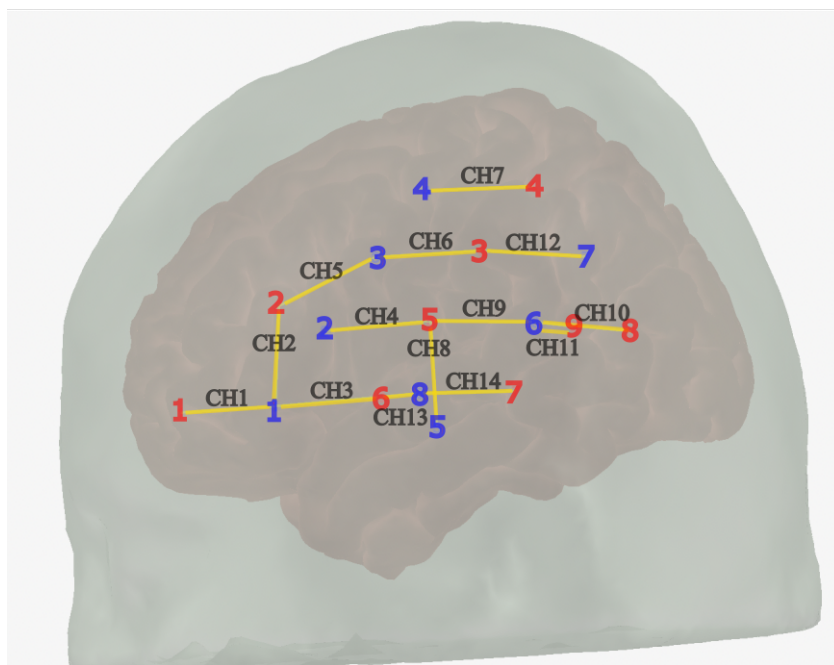


Figure 3.1: Channel Definition

Results

In the following figures. Channels with invalid SCI would not be taken into consideration, and hence would not be shown. Measurements in all channels were plotted in the same scale except for the two short channels marked in thicker outlines. In all our measurements, the changes in the dynamic hemoglobin response were significantly less in the short channels by more than a magnitude.

Our regions of interest (ROI) are defined as the following figure. The auditory cortex is in particular of our interest. Hence, channel 4, channel 8, and channel 9 together formed one region (ROI 2). The rest of the channels formed ROI 1. It is of our interest to compare how the response of the auditory cortex differ from the rest of the left brain hemisphere.

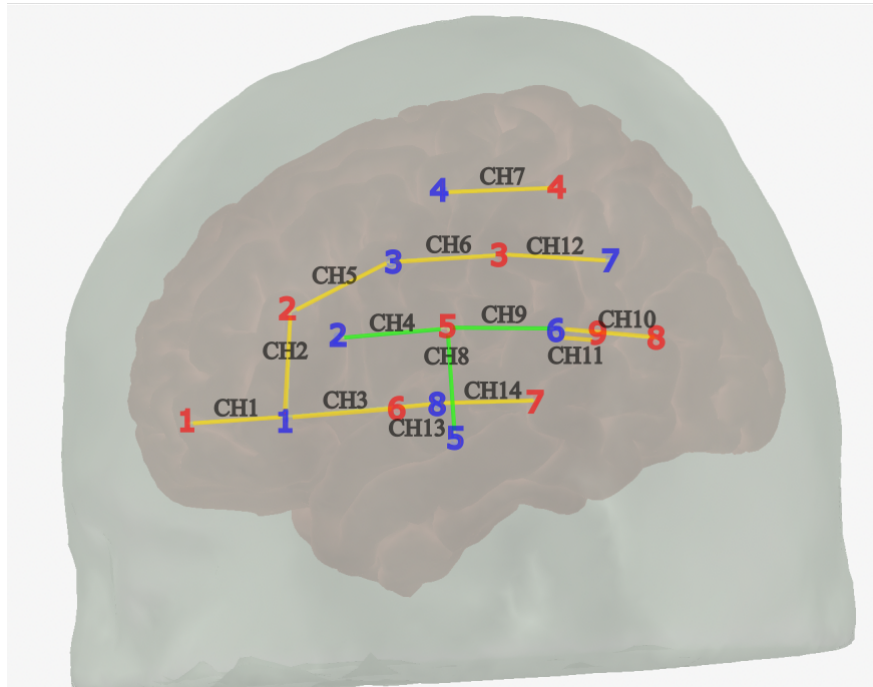


Figure 3.2: ROI Definition

3.1 Participant 3

3.1 Participant 3

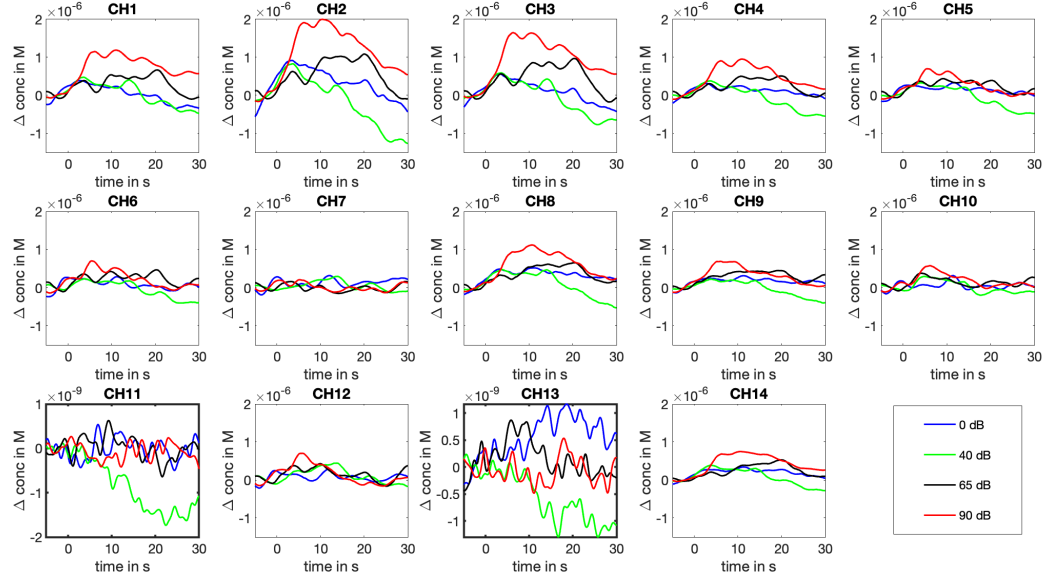


Figure 3.3: HbO Measurement from participant 3.

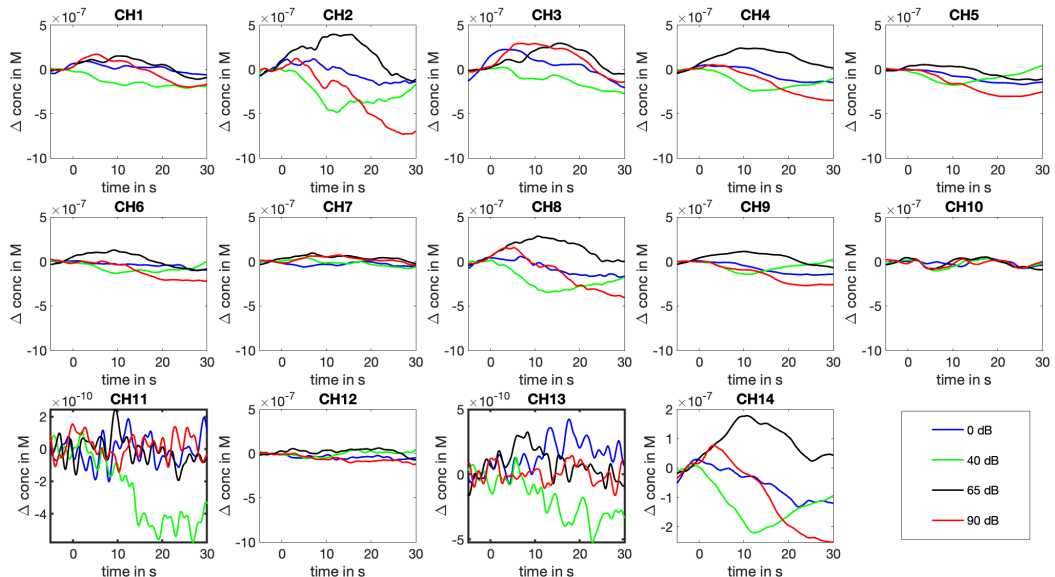


Figure 3.4: HbR Measurement from participant 3.

Results

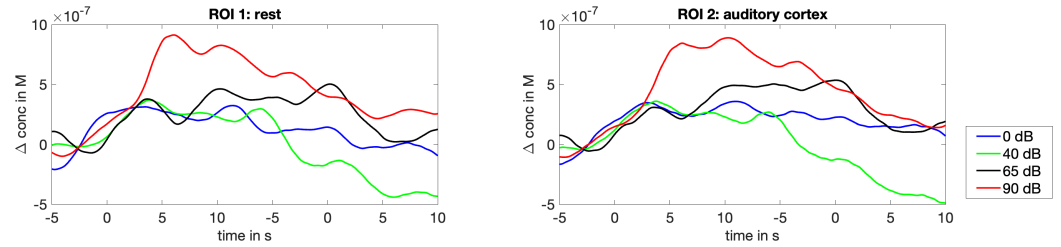


Figure 3.5: ROI Measurement from participant 3.

The results from this participant was the closest one to the results reported by Weder et al. For the oxygenated hemoglobin HbO waveform morphology, tonic response could be observed in channel 1, 2, and 3, and phasic response could be observed in channel 10 and 12.

3.2 Participant 5

3.2 Participant 5

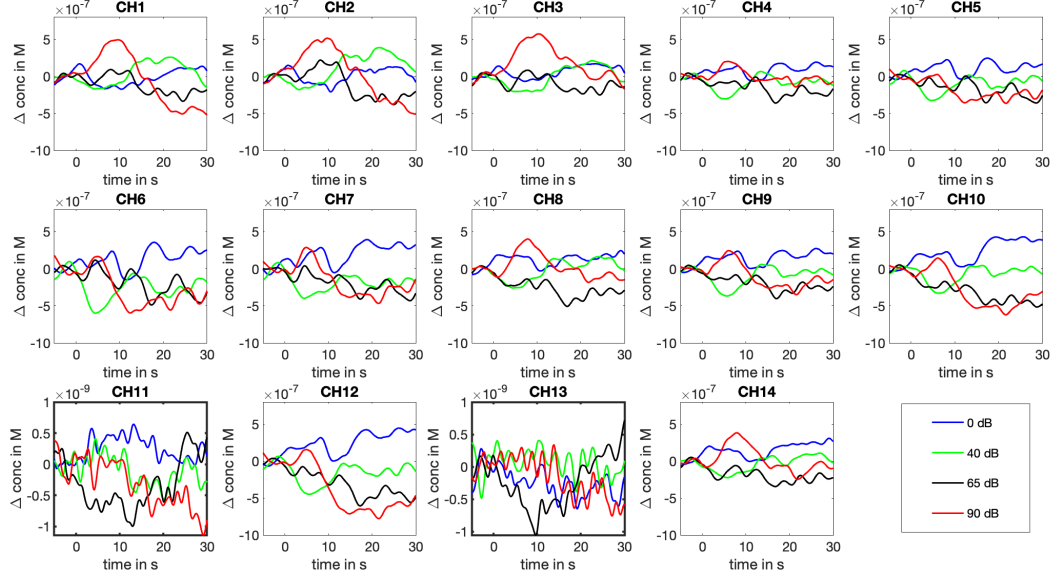


Figure 3.6: HbO Measurement from participant 5.

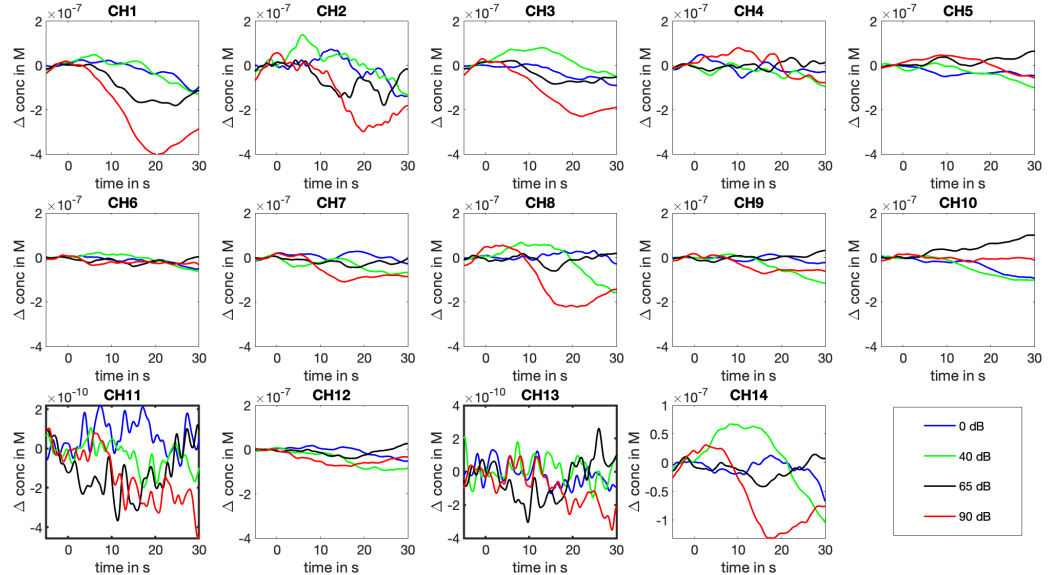


Figure 3.7: HbR Measurement from participant 5.

Results

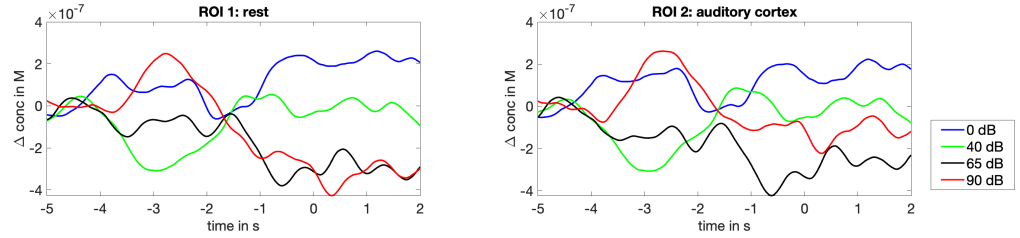


Figure 3.8: ROI Measurement from participant 5.

For the oxygenated hemoglobin (HbO_2) waveform, there were significantly larger on-sets for the 90 dB sound stimuli in Channel 1, 2, and 3, i.e. around the Broca's area.

Apart from this, the waveforms for deoxygenated hemoglobin (HbR), were also quite different from the ones Weder et al 2018. reported. For the loudest sound stimuli, channels overlying the caudal superior temporal gyrus and channels over Broca's area showed clear phasic response.

3.3 Participant 6

3.3 Participant 6

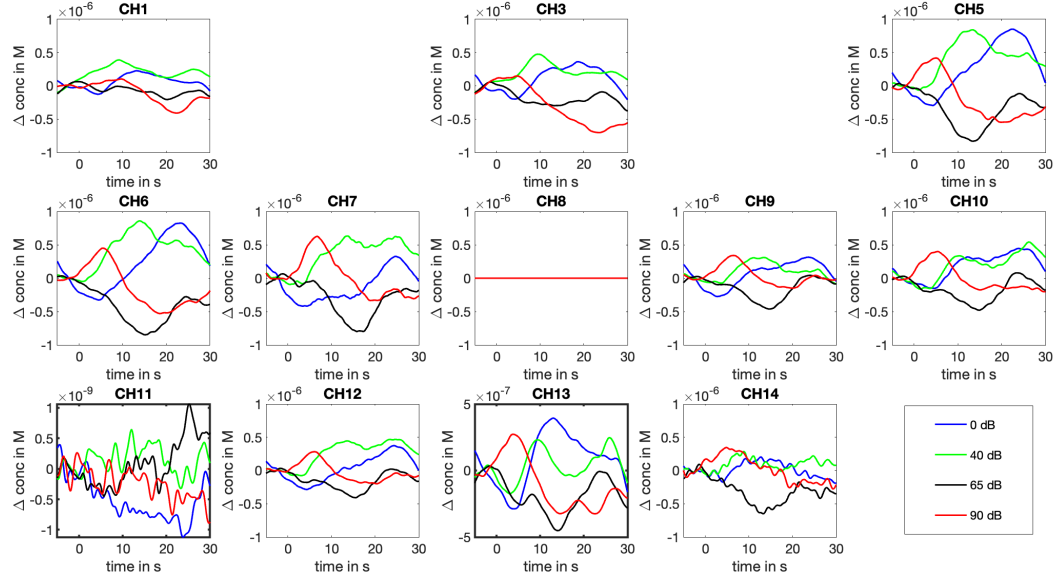


Figure 3.9: HbO Measurement from participant 6.

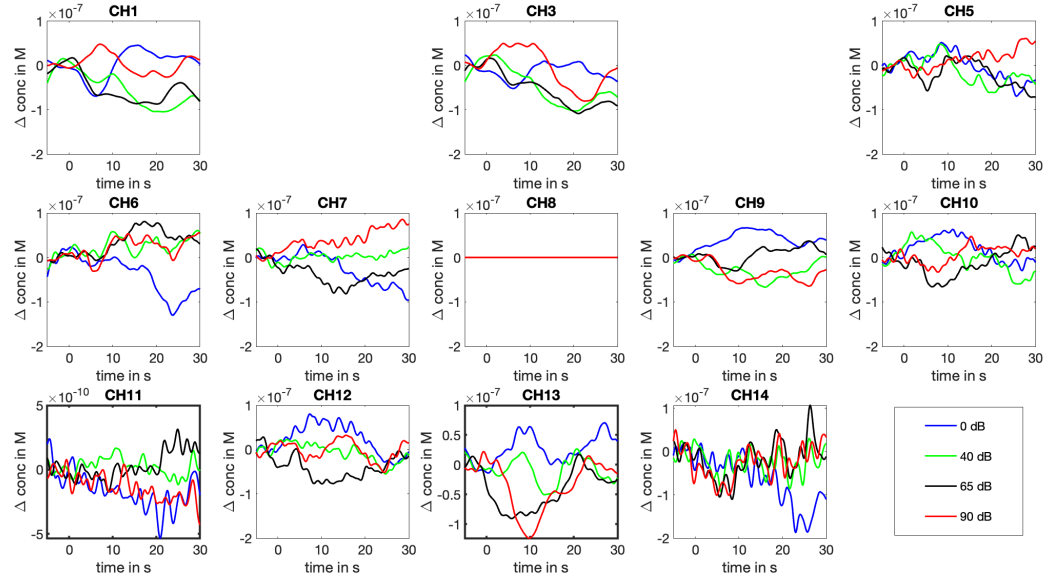


Figure 3.10: HbR Measurement from participant 6.

Results

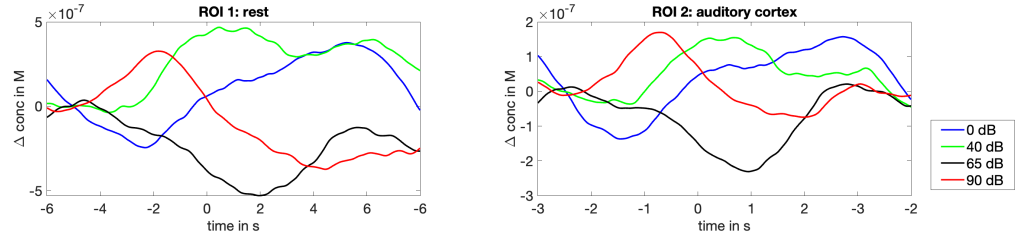


Figure 3.11: ROI Measurement from participant 6.

For the oxygenated hemoglobin, HbO waveform, the loudest sound stimuli resulted in phasic response for almost all the channels. In addition, it also resulted in faster on-set compared with other stimuli of lower sound pressure levels.

On the other hand, as for the deoxygenated hemoglobin, HbR response, results from multiple channels appeared to be noisy even if the SCI values were already above the suggested threshold.

3.4 Participant 7

3.4 Participant 7

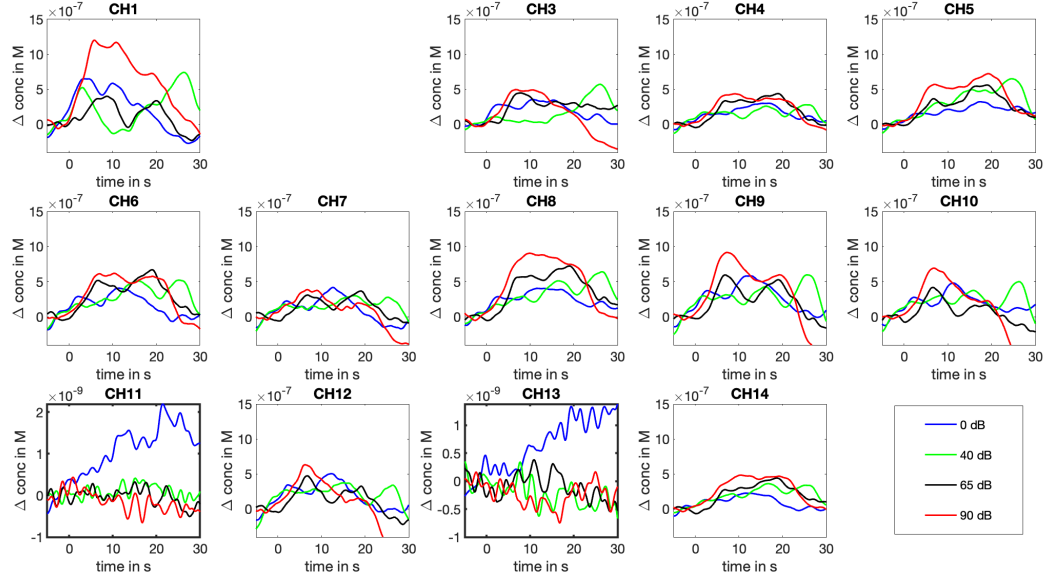


Figure 3.12: HbO Measurement from participant 7.

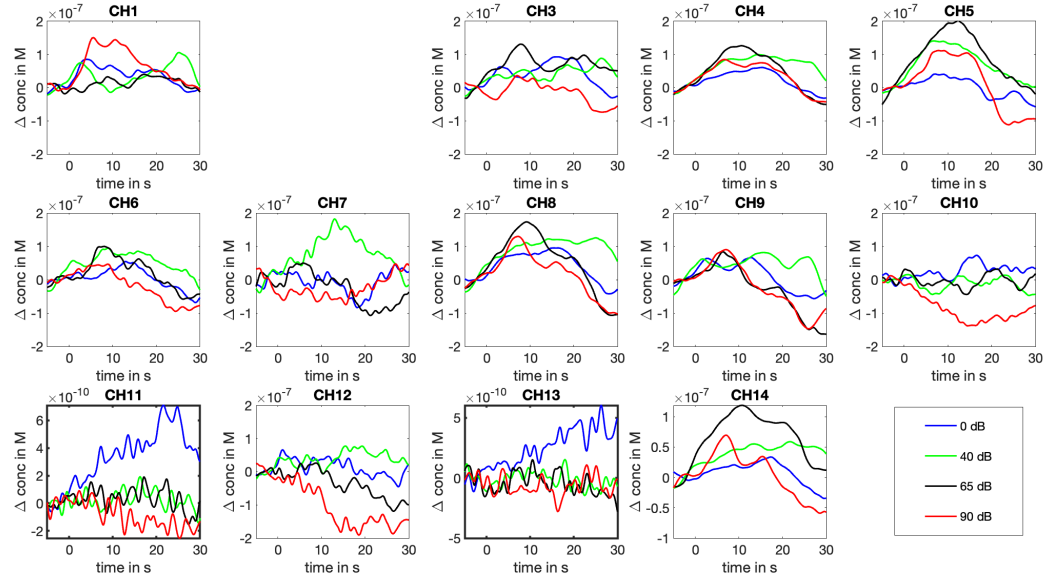


Figure 3.13: HbR Measurement from participant 7.

Results

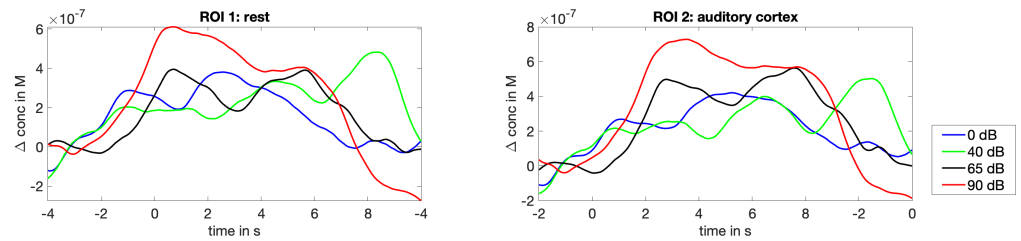


Figure 3.14: ROI Measurement from participant 7.

The results from this participant are rather indeterminant to differentiate between response to different sound pressure levels.

3.5 Participant 4

3.5 Participant 4

There were also some poor measurements even though the SCI is above the threshold 0.75. For example, in our case of participant 4. One possible reason can be due to the thick dark hair of the participant. Light absorption can affect the result greatly.

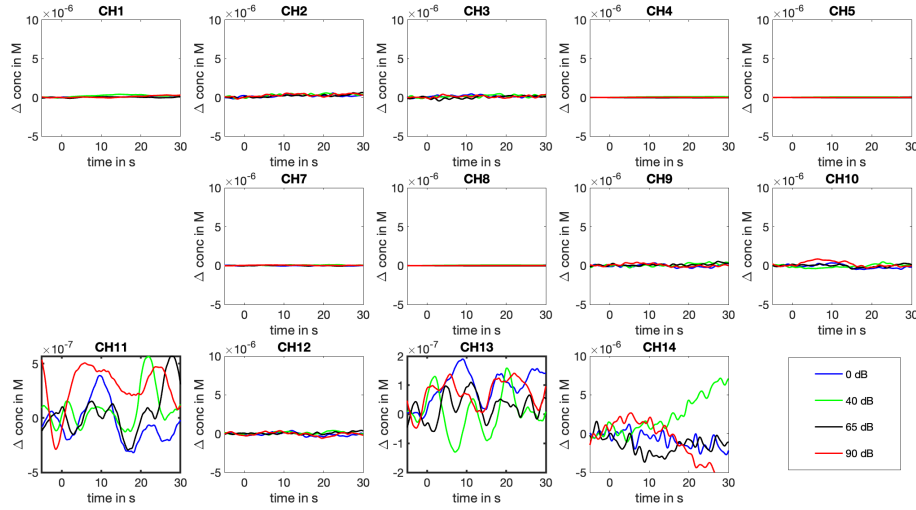


Figure 3.15: HbO Measurement from participant 4.

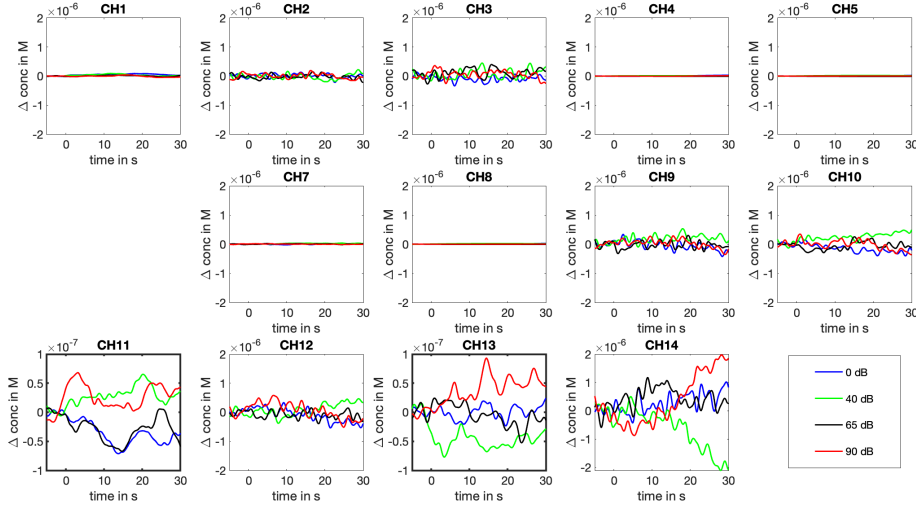


Figure 3.16: HbR Measurement from participant 4.

Results

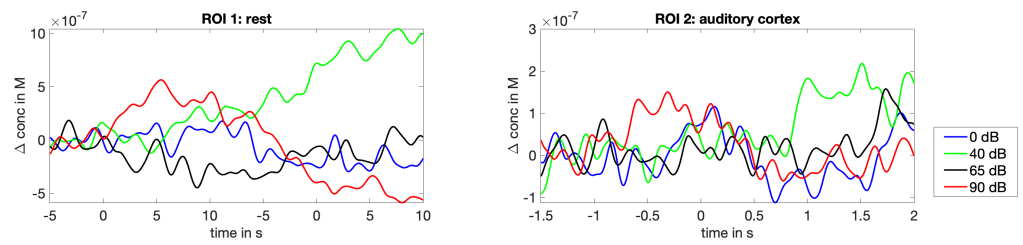


Figure 3.17: ROI Measurement from participant 4.

3.6 Participant 8

3.6 Participant 8

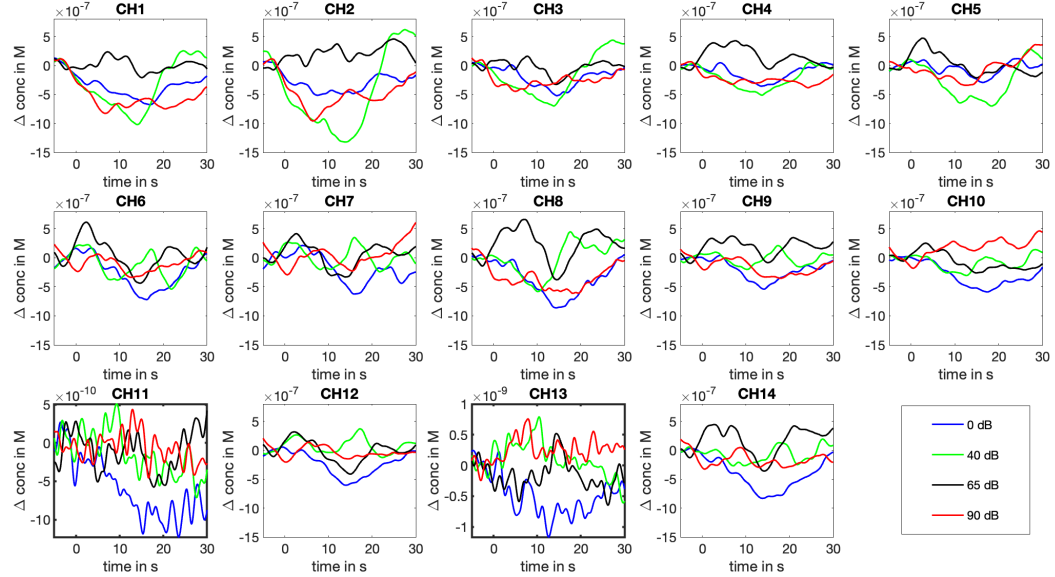


Figure 3.18: HbO Measurement from participant 8. Silent comparison

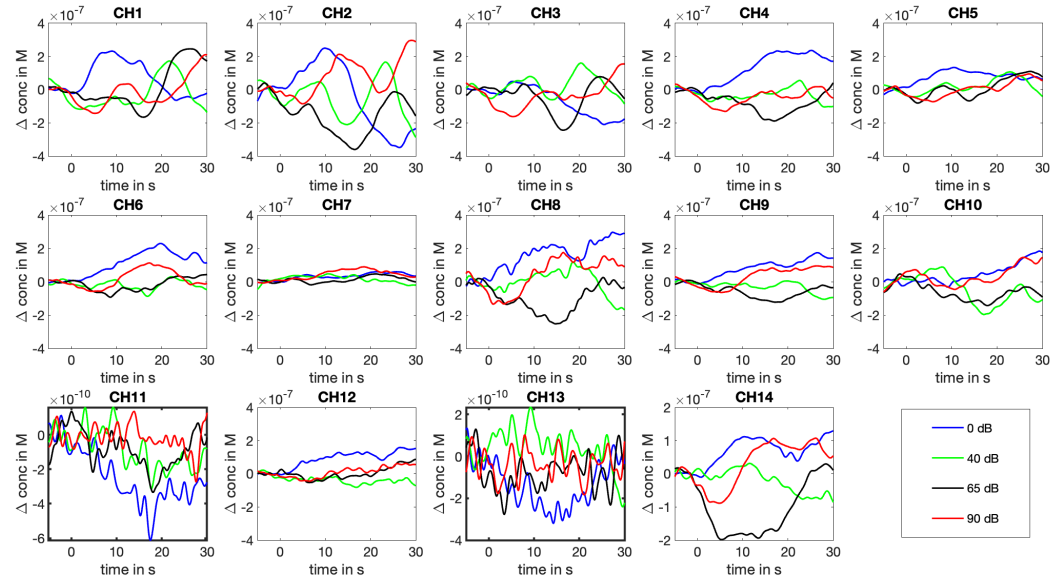


Figure 3.19: HbR Measurement from participant 8. Silent comparison

Results

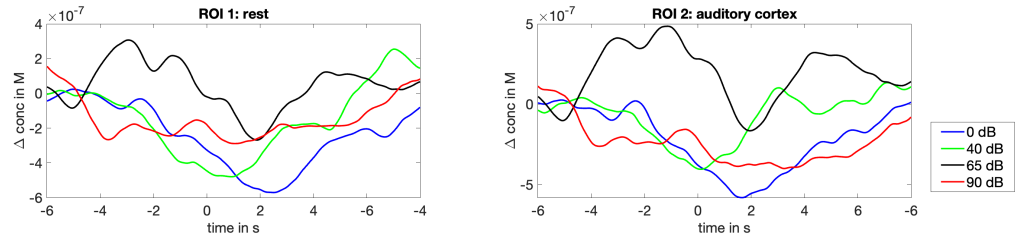


Figure 3.20: ROI Measurement from participant 8. Silent comparision.

This participant was given only silence stimuli. No pattern could be concluded for the measured waveform morphology. Nonetheless, it's noteworthy to know that even if there are almost no visual and sound stimuli, dynamic hemoglobin response still exists.

Chapter 4

Discussion

4.1 Waveform Morphology

The results we got for the waveform morphologies did not speak entirely with the results that Weder et al. 2018 reported. In most of the cases, larger sound pressure level did result in greater positive change of oxygenated hemoglobin concentration, or in other words, greater negative change in deoxygenated hemoglobin concentration. However, the results were not consistent between participants. The separation between different sound pressure levels could not be clearly seen. Apart from the results with the loudest audio stimuli, responses from other quieter audio stimuli were rather indistinguishable. Moreover, regarding the type of responses we measured from different regions of the left brain hemisphere, phasic response could be observed from the channels over the supramarginal superior temporal gyrus from most of the participants. However, only from some of the participants, channels over Broca's area could show a broad tonic pattern as Weder et al. 2018 described.

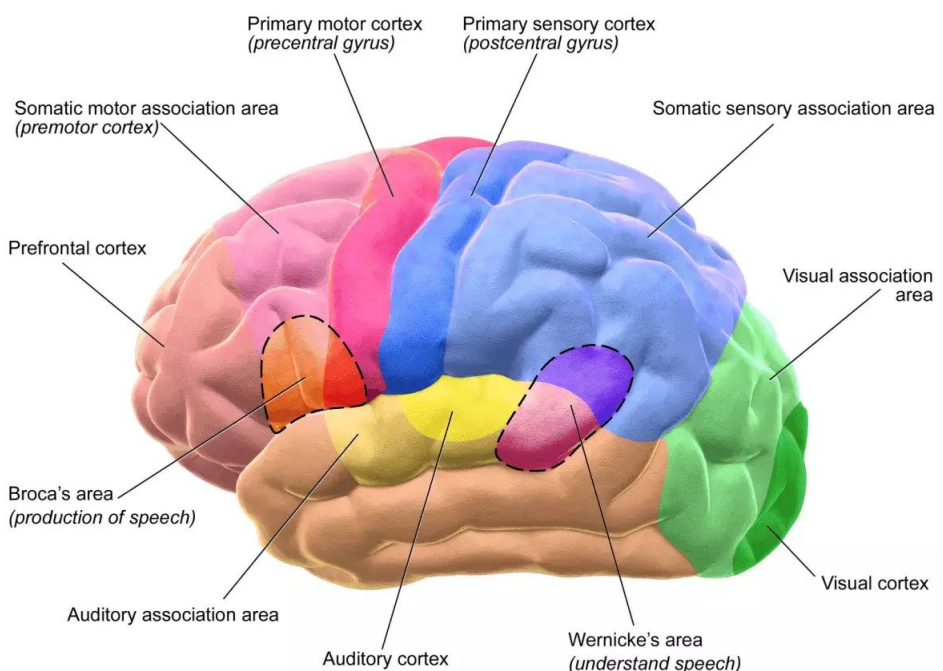
4.2 Regional Analysis

In comparison to the research from Weder et al. 2018, we chose a different approach to define our region of interest. Instead of first looking at the results and grouping different regions according to similar waveforms, we were more interested to know how the responses from the auditory cortex would be compared with other regions of the measured left brain hemisphere, so we grouped the three channels over the caudal superior temporal gyrus as one region (ROI 2), and the rest of the channels as another region (ROI 1).

The auditory cortex 4.1 was our interest of this study. It is around the caudal superior temporal gyrus. We compared the hemoglobin response from

Discussion

the three channels over the auditory cortex with all the other channels lying on the rest of the measured left brain hemisphere. The waveform morphology of the auditory cortex is very similar to the counterparts of the rest of the measured parts. In other words, the dynamic hemoglobin response of the auditory cortex represents that of the entire left brain hemisphere fairly well.



Source: <https://human-memory.net/sensory-cortex/>

Figure 4.1: Motor and Sensory Regions of the Cerebral Cortex

4.3 Device Limitation and fNIRS Testing Conditions

There could be several factors that potentially caused the results from this project to vary from that Weder et al. 2018 reported. First, we used the device Brite23. It is also a continuous-wave fNIRS device. The sources emitted light of slightly different wavelengths, which are 757 nm and 843 nm, whereas Weder et al. 2018 uses the device (NIRScout, NIRX, Germany) which sources emitted light of wavelengths 760 nm and 850 nm. Additionally as for the fNIRS testing procedure, we could have also improved on several things. To begin with, a darker sound booth would be more suitable. In

4.4 Data Processing

our setup, the testing was also performed in a sound booth, but with normal light condition. Still, if the lighting was dimmer, there could be less noise in the hemoglobin response from visual stimulation. In addition, it would make sense to stabilize the participant's neck with a neck cushion. Not only would it be more comfortable for the participants during the measurement. Movement artifacts could also be reduced. Moreover, by including breaks in between can help participant maintain better attention.

Also, from our measurements, data from female participants with long hair had worse data quality. In our configuration, since we were only measuring the left brain hemisphere. First asking the participant to put the hair to the right side made it easier to put the cap on. Sometimes when the participants had thick long hair, trying to put the hair aside can be a futile attempt, but it was easier when they first put the hair to the other side. Last but not least, we would be curious to know how would the hemoglobin response from more people be like. If possible, more participants should be measured so the results from the project can be more credible. For example, participants of different ages and every gender and race would be desirable for this hearing research. Besides, other than only measure normal-hearing people, it would also be of our great interest to measure some cochlear implant users and compare the results together.

4.4 Data Processing

Our measured data was processed with a modified approach. In the research from Weder et al. 2018, data pre-processing and analysis was executed in MATLAB and SPSS (version 24, IBM Corp., USA). They combined custom-made MATLAB scripts with Homer2 functions. On the other hand, the newer Homer3 with our MATLAB script in this study. Judging from the varying individual results, group analysis or statistical analysis will not be applicable in this case. Hence, the software program for statistical analysis, SPSS, was not used in this project. Furthermore, the differential pathlength factor (DPF) for each participant was calculated from their age. The resultant HbO and HbR concentration was estimated with the correction factor, whereas Weder et al. 2018 did not mention how they chose or calculated the DPF values.

Discussion

4.5 Loudness Perception

In this project, results from individuals varied much. Although in hearing research, response from normal-hearing participants should be similar and reproducible, it is also well-known that, even between normal-hearing listeners, considerable differences still exist in loudness perceptions Garnier et al. [1999]. A more recent research Weder et al. [2020] was conducted in detail, and showed that Brain activation in response to different stimulus intensities is more reliant upon individual loudness sensation than the physical stimulus properties. Therefore, the authors suggested that loudness estimates should be examined when interpreting results, especially when it comes to measurements using different auditory stimulus intensities. Different loudness perception can explain the varying results from individual participants.

4.6 Audio Stimuli

ICRA noises were chosen as the stimuli in this study because it is believed to be able to activate broad cortical auditory areas. However, some other researches were able to detect differences in cortical responses to speech of different intelligibility. Pollonini et al. 2013 found that normal speech evoked stronger responses within the auditory cortex than distorted speech did, and environmental sounds produced the least cortical activation. ICRA noises are amplitude-modulated noises, are completely unintelligible, and thus, belong to the distorted-speech category. Although ICRA noises may be able to activate broader cortical auditory areas than simple static stimulus, normal speech can perhaps produce even stronger responses within auditory cortex, according to Pollonini et al. 2013. In addition, by providing intelligible normal speech as a stimuli rather than unintelligible noise, the measurement process can be less boring for the participants. They can then be more compliant and thus maintain better attention to actively listen to the soundtracks.

4.7 Language Processing in Human Brains

One primary goal of fNIRS researches is to improve a patient's ability to discriminate speech. In many researches, topics associated with hearing and language processing were investigated. However, language perception and processing in human brain do not have to be involved with audio stimuli. Visual-only speech can also activate language processing in the human brain. Shader et al. 2021 used both auditory-only and visual-only connected speech

4.8 Laterality of Brain Activation

as stimuli in their research. Their results suggested that Heschl's gyrus may be the most advantageous location for identifying hemodynamic responses to complex auditory speech signals using fNIRS, for measuring responses to visual speech with fNIRS, regions corresponding to the facial processing pathway in occipital lobe can be more advantageous.

4.8 Laterality of Brain Activation

In this study, the fNIRS optodes were all placed on the left brain hemisphere, since according to Frost et al. 1999, language processing is strongly left lateralized. Nonetheless, from other papers, different results were observed and did not speak with the conclusion from Frost et al. 1999. For example, the data from Pollonini et al. 2013 is more responsive to changes in activation within the right hemisphere. Belin et al. 2000 showed that the voice-selective regions can be found bilaterally along the upper bank of STS. Shader et al. Shader et al. [2021] also measured relatively symmetrical patterns across both hemispheres. Hence, if it is more advantageous to measure the left hemisphere for cortical response to audiometric stimuli with fNIRS remains till this point a question to be answered.

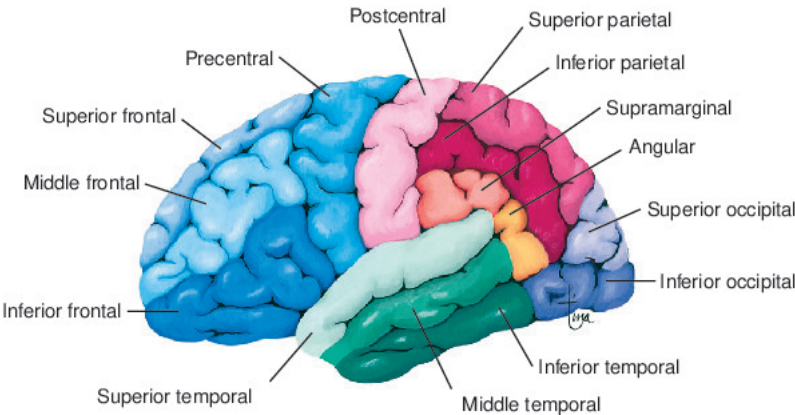
4.9 Depth and Location of Cortical Response

The depth of cortical response to complex auditory speech signals can also greatly affect the fNIRS measurements. Strangman et al. 2013 demonstrated that sensitivity in depth decreases exponentially and diminishing returns appear to begin around 40 to 50 mm source-detector separations.

The left inferior frontal gyrus 4.2, or more specifically Broca's area 4.1 is implicated in higher-level linguistic processing Belin et al. [2000]. While in some studies Wijayasiri et al. [2017] Zhou et al. [2018], significant cortical activity in response to auditory speech signals in this region can be detected, it was not always the case Mushtaq et al. [2019]. The studies that observed significant activation in the frontal region used fMRI or a combination of fMRI and fNIRS. It is possible that speech-evoked activity in the inferior frontal gyrus is isolated to the deeper cortical areas, so it's less likely to be detected with fNIRS. Different neuro-imagining methods can also explain why some studies Frost et al. [1999] reported language processing to be left-lateralized whereas in other studies Shader et al. [2021], opposite results were observed. It is possible that speech-evoked activities is related to the deeper cortical areas in the left hemisphere while the stimuli evoked responses in

Discussion

more superficial areas of the right cortex, making them more easily detected by fNIRS.



Source: <https://www.tabers.com/tabersonline/view/Tabers-Dictionary/734639/all/gyrus>

Figure 4.2: Gyrus

4.10 HbR and HbO Data

Most fNIRS studies only present HbO data Ferrari and Quaresima [2012], since it has a lower noise level, and thus more obvious responses can be observed. However, with our system, no significant difference was found regarding the HbO and HbR noise levels for most of the participants. Only some channels were measured with higher noise levels for the HbR data collected from participant 6. Unlike what Weder et al. 2018 presented in their paper, we were surprised to be able to measure comparably large HbO and HbR responses.

Chapter 5

Conclusion and Future Prospectives

This study aims to confirm and reproduce the results from Weder et al. 2018. With the limited devices, we made our measurement conditions, i.e. optode template configuration and audio sound stimuli as similar as those of the previous research from Weder et al. 2018 as possible.

Our results were not completely as expected. Few common patterns could be found between participants. Therefore, we analysed the results from each individual participant and compared these with the results Weder et al. 2018 provided. Variables that might have potentially affected the results of the study were investigated with a thorough literature review.

Other than purely reproducing the results from the one main paper Weder et al. [2018], this study also take other related research into consideration. We studied and considered the effect of different audio stimuli, individual perception of loudness of the sound, depth, laterality and location of the cortical activation. By taking advantage of previous fMRI studies Belin et al. [2000] Belin et al. [2002] Hall et al. [2001] Frost et al. [1999], we compared the laterality of cortical activation in this study and previous researches. Building upon the presumption from earlier researches and our measurement data, we also concluded that the cortical activation from audio stimuli is possibly deeper for some participants in the audio cortex. Additionally other than merely taking the HbO data for analysis, the magnitude and noise of the measured HbR data was also compared with the counterparts of the HbO data.

Appendix A

Acronym

Acronyms

BOLD Blood-oxygen-level-dependent. 2

CW-NIRS continuous wave near-infrared spectroscopy. 3

DPF differential path length factor. 3

fMRI functional magnetic resonance imaging. 1, 3, 4

fNIRS functional near-infrared spectroscopy. 1–4, 33

HbO oxygenated hemoglobin. 20, 22

HbR deoxygenated hemoglobin. 20, 22

mBLL modified Beer-Lambert law. 3

STS superior temporal sulcus. 4, 33

Appendix B

List of Figures

List of Figures

1.1 Some Anatomical Terminology. The terms anterior, posterior, superior, and inferior refer to the long axis of the body, which is straight. Therefore, these terms indicate the same direction for both the forebrain and the brainstem. In contrast, the terms dorsal, ventral, rostral, and caudal refer to the long axis of the central nervous system.	5
2.1 Probe design from Weder et al. 2018	7
2.2 Probe design in this research. Shown in AtlasViewer 2015 . The red numbers represent the light sources and the blue numbers represent the detector. Channels are shown in yellow lines.	7
2.4 Manufacturing process of the cap	8
2.5 Finished cap on dummy	8
2.3 SDgui interface and optode coordinates.	8
2.6 Flow Chart of Data Processing	11
2.7 Age dependence of DPF. From Duncan et al.	13
2.8 Distribution of SCI values.	14
3.1 Channel Definition	15
3.2 ROI Definition	16
3.3 HbO Measurement from participant 3.	17
3.4 HbR Measurement from participant 3.	17
3.5 ROI Measurement from participant 3.	18
3.6 HbO Measurement from participant 5.	19
3.7 HbR Measurement from participant 5.	19
3.8 ROI Measurement from participant 5.	20
3.9 HbO Measurement from participant 6.	21
3.10 HbR Measurement from participant 6.	21
3.11 ROI Measurement from participant 6.	22
3.12 HbO Measurement from participant 7.	23
3.13 HbR Measurement from participant 7.	23

List of Figures

3.14	ROI Measurement from participant 7	24
3.15	HbO Measurement from participant 4	25
3.16	HbR Measurement from participant 4	25
3.17	ROI Measurement from participant 4	26
3.18	HbO Measurement from participant 8. Silent comparison . . .	27
3.19	HbR Measurement from participant 8. Silent comparison . . .	27
3.20	ROI Measurement from participant 8. Silent comparision. . .	28
4.1	Motor and Sensory Regions of the Cerebral Cortex	30
4.2	Gyrus	34

Appendix C

List of Tables

List of Tables

2.1 Demographic information of the study participants.	6
--	---

Bibliography

- Aasted, C. M., Yücel, M. A., Cooper, R. J., Dubb, J., Tsuzuki, D., Becerra, L., Petkov, M. P., Borsook, D., Dan, I., and Boas, D. A. (2015). Anatomical guidance for functional near-infrared spectroscopy: AtlasViewer tutorial. *Neurophotonics*, 2(2):020801.
- Arridge, S. R., Cope, M., and Delpy, D. T. (1992). The theoretical basis for the determination of optical pathlengths in tissue: temporal and frequency analysis. *Physics in Medicine and Biology*, 37(7):1531–1560.
- Belin, P., Zatorre, R., and Ahad, P. (2002). Human temporal-lobe response to vocal sounds. *Brain research. Cognitive brain research*, 13:17–26.
- Belin, P., Zatorre, R., Lafaille, P., Ahad, P., and Pike, B. (2000). Voice-selective areas in human auditory cortex. *Nature*, 403:309–12.
- Chan, D., Fourcin, A., Gibbon, D., Granstrom, B., Hucvale, M., George, K., Kvale, K., Lamel, L., Lindberg, B., Moreno, A., Mouropoulos, J., and Senia, F. (1995). Eurom - a spoken language resource for the eu. *Proc. Eurospeech*, 1.
- Clark, B. A. (2000). First-and second-language acquisition in early childhood.
- Delpy, D. T., Cope, M., van der Zee, P., Arridge, S., Wray, S., and Wyatt, J. (1988). Estimation of optical pathlength through tissue from direct time of flight measurement. *Physics in Medicine and Biology*, 33(12):1433–1442.
- Dreschler, W., Herschuure, H., Ludvigsen, C., and Westermann, S. (2001). Icra noises: Artificial noise signals with speech-like spectral and temporal properties for hearing aid assessment. *Audiology*, 40:148–157.
- Duncan, A., Meek, J., Clemence, M., Elwell, C. E., Fallon, P., Tyszczuk, L., Cope, M., and Delpy, D. T. (1996). Measurement of cranial optical path length as a function of age using phase resolved near infrared spectroscopy. *Pediatric Research*, 39:889–894.

Bibliography

- Ferrari, M. and Quaresima, V. (2012). A brief review on the history of human functional near-infrared spectroscopy (fnirs) development and fields of application. *NeuroImage*, 63(2):921–935.
- Frost, J. A., Binder, J. R., Springer, J. A., Hammeke, T. A., Bellgowan, P. S., Rao, S. M., and Cox, R. W. (1999). Language processing is strongly left lateralized in both sexes. evidence from functional MRI. *Brain*, 122 (Pt 2):199–208.
- Garnier, S., Micheyl, C., Berger-Vachon, C., and Collet, L. (1999). Effect of signal duration on categorical loudness scaling in normal and in hearing-impaired listeners. *Audiology : official organ of the International Society of Audiology*, 38:196–201.
- Hall, D., Haggard, M., Summerfield, A., Akeroyd, M., Palmer, A., and Bowtell, R. (2001). Functional magnetic resonance imaging measurements of sound-level encoding in the absence of background scanner noise. *The Journal of the Acoustical Society of America*, 109:1559–70.
- Huppert, T. J., Diamond, S. G., Franceschini, M. A., and Boas, D. A. (2009). Homer: a review of time-series analysis methods for near-infrared spectroscopy of the brain. *Appl. Opt.*, 48(10):D280–D298.
- Jöbsis, F. F. (1977). Noninvasive, infrared monitoring of cerebral and myocardial oxygen sufficiency and circulatory parameters. *Science*, 198(4323):1264–1267.
- Molavi, B. and Dumont, G. A. (2012). Wavelet-based motion artifact removal for functional near-infrared spectroscopy. *Physiological Measurement*, 33(2):259–270.
- Mushtaq, F., Wiggins, I., Kitterick, P., Anderson, C., and Hartley, D. (2019). Evaluating time-reversed speech and signal-correlated noise as auditory baselines for isolating speech-specific processing using fnirs. *PLOS ONE*, 14:e0219927.
- Newport, E. L. (1990). Maturational constraints on language learning. *Cognitive Science*, 14(1):11–28.
- Pelphrey, K. A. (2013). *Blood-Oxygen-Level-Dependent (BOLD) Signal*, pages 465–466. Springer New York, New York, NY.

Bibliography

- Pollonini, L., Olds, C., Abaya, H., Bortfeld, H., Beauchamp, M., and Oghalai, J. (2013). Auditory cortex activation to natural speech and simulated cochlear implant speech measured with functional near-infrared spectroscopy. *Hearing research*, 309.
- Robinshaw, H. M. (1995). Early intervention for hearing impairment: Differences in the timing of communicative and linguistic development. *British Journal of Audiology*, 29(6):315–334. PMID: 8861408.
- Shader, M., Luke, R., Gouailhardou, N., and McKay, C. (2021). The use of broad vs restricted regions of interest in functional near-infrared spectroscopy for measuring cortical activation to auditory-only and visual-only speech. *Hearing Research*, 406:108256.
- Strangman, G. E., Li, Z., and Zhang, Q. (2013). Depth sensitivity and source-detector separations for near infrared spectroscopy based on the colin27 brain template. *PLOS ONE*, 8(8):1–13.
- Swinehart, D. F. (1962). The beer-lambert law. *Journal of Chemical Education*, 39(7):333.
- Weder, S., Shoushtarian, M., Olivares, V., Zhou, X., Innes-Brown, H., and McKay, C. (2020). Cortical fnirs responses can be better explained by loudness percept than sound intensity. *Ear and Hearing*, 41:1.
- Weder, S., Zhou, X., Shoushtarian, M., Innes-Brown, H., and McKay, C. (2018). Cortical processing related to intensity of a modulated noise stimulus-a functional near-infrared study. *J. Assoc. Res. Otolaryngol.*, 19(3):273–286.
- Wijayasiri, P., Hartley, D., and Wiggins, I. (2017). Brain activity underlying the recovery of meaning from degraded speech: A functional near-infrared spectroscopy (fnirs) study. *Hearing Research*, 351.
- Yoshinaga-Itano, C., Sedey, A., Coulter, D., and Mehl, A. (1998). Language of early- and later-identified children with hearing loss. *Pediatrics*, 102:1161–71.
- Zhou, X., Seghouane, A.-K., Shah, A., Innes-Brown, H., Cross, W., Litovsky, R., and McKay, C. M. (2018). Cortical speech processing in postlingually deaf adult cochlear implant users, as revealed by functional near-infrared spectroscopy. *Trends in Hearing*, 22:2331216518786850. PMID: 30022732.

Bibliography

Erklärung der Selbstständigkeit

Hiermit versichere ich, die vorliegende Arbeit selbstständig verfasst und keine anderen als die angegebenen Quellen und Hilfsmittel benutzt sowie die Zitate deutlich kenntlich gemacht zu haben.

.....
Ort, Datum

Pei-Yi Lin